

# Eukaryotic Translation Initiation Factor 3, Subunit a, Regulates the Extracellular Signal-Regulated Kinase Pathway

Tian-Rui Xu,<sup>a</sup> Rui-Fang Lu,<sup>a</sup> David Romano,<sup>b</sup> Andrew Pitt,<sup>a\*</sup> Miles D. Houslay,<sup>a</sup> Graeme Milligan,<sup>a</sup> and Walter Kolch<sup>b,c</sup>

Institute of Neuroscience and Psychology, College of Medical, Veterinary and Life Sciences, University of Glasgow, Glasgow, United Kingdom<sup>a</sup>; Systems Biology Ireland, University College Dublin, Dublin, Ireland<sup>b</sup>; and Conway Institute, University College Dublin, Dublin, Ireland<sup>c</sup>

**The extracellular signal-regulated kinase (ERK) pathway participates in the control of numerous cellular processes, including cell proliferation. Since its activation kinetics are critical for its biological effects, they are tightly regulated. We report that the protein translation factor, eukaryotic translation initiation factor 3, subunit a (eIF3a), binds to SHC and Raf-1, two components of the ERK pathway. The interaction of eIF3a with Raf-1 is increased by  $\beta$ -arrestin2 expression and transiently decreased by epidermal growth factor (EGF) stimulation in a concentration-dependent manner. The EGF-induced decrease in Raf-1–eIF3a association kinetically correlates with the time course of ERK activation. eIF3a interferes with Raf-1 activation and eIF3a downregulation by small interfering RNA enhances ERK activation, early gene expression, DNA synthesis, expression of neuronal differentiation markers in PC12 cells, and Ras-induced focus formation in NIH 3T3 cells. Thus, eIF3a is a negative modulator of ERK pathway activation and its biological effects.**

The extracellular signal-regulated kinase (ERK) pathway is involved in many fundamental cellular processes, including cell proliferation and transformation (5, 11). The activation sequence of the core components of the pathway is well characterized (32, 39). The pathway is typically activated by receptor tyrosine kinases, such as the epidermal growth factor (EGF) receptor (EGFR), which autophosphorylate at their intracellular kinase domains upon ligand binding. These phosphotyrosines serve as docking sites for adaptor proteins and signal transducers which activate the downstream pathways that mediate the biological effects of the ligands. The ERK pathway is initiated by the translocation of the guanine nucleotide exchange factor (GEF) SOS from the cytosol to the plasma membrane via the adaptor proteins SHC and Grb2 binding to specific phosphotyrosines at the EGFR. SOS then activates Ras, which binds to Raf kinases recruiting them to the membrane for activation. Raf activation is a complex process that is still not fully elucidated, and slightly different between the three Raf isoforms A-Raf, B-Raf, and Raf-1. A critical step in Raf-1 activation is the Ras-induced dephosphorylation of the inhibitory phospho-S259, which is required for the subsequent phosphorylation of the key activating site S338 (12, 13). Active Raf-1 phosphorylates MEK, which in turn phosphorylates ERK. ERK has >150 substrates in the cytosol and nucleus (45). This large number of substrates enables the pathway to carry out its highly pleiotropic functions, although it is still rather enigmatic as to how specificity in signaling and biological responses is produced. Nevertheless, it is thought that the activation kinetics, spatial organization, cross talk, and binding to scaffold proteins contribute to the generation of signaling specificity (5, 39). Thus, although the core pathway is well mapped, identification and analysis of the proteins that modulate these parameters is required in order to understand the functional diversity of the pathway.

We report here the identification of eukaryotic translation initiation factor 3, subunit a (eIF3a), as a protein that modulates the activation kinetics of the ERK pathway. eIF3a (also called eIF3 $\theta$ , p150, and p170) is a component of eIF3, a multisubunit factor involved in mRNA translation (7, 17, 22). eIF3 participates in forming the preinitiation complex and preventing the premature

binding of the 40S to the 60S ribosomal subunits (17, 22). eIF3a can regulate cell cycle progression and proliferation, presumably by controlling the translation of mRNAs encoding the cell cycle inhibitor p27<sup>Kip1</sup> and the M2 subunit of ribonucleotide reductase, which is a rate-limiting enzyme in DNA synthesis (15, 16). Similarly, overexpression of certain eIF3 subunits, including eIF3a, can transform NIH 3T3 cells by enhancing global protein synthesis and, in particular, the synthesis of proteins that stimulate proliferation, such as cyclin D1, c-Myc, fibroblast growth factor 2, and ornithine decarboxylase (46). Intriguingly, however, in mammalian cells eIF3a is not deemed essential for the function of eIF3, and not all of eIF3a is associated with ribosomes, indicating that it may have functions unrelated to protein translation (36). Indeed, eIF3a has been reported to bind to actin (34), cytokeratin 7 (27), and microtubules (20, 37) and the TrkA receptor (30), although the functional consequences of these interactions remain to be ascertained.

We have found that eIF3a can regulate the ERK pathway by binding to Raf-1. Critically, the interaction with Raf-1 is enhanced by the signaling scaffold protein  $\beta$ -arrestin2 and, in doing so, it interferes with Raf-1 activation. Consistent with these observations, the downregulation of eIF3a results in prolonged ERK activation, induction of the nuclear ERK target c-Fos, enhanced proliferation, transformation in NIH 3T3 cells, and induction of neuronal differentiation markers in PC12 cells.

Received 9 June 2011 Returned for modification 28 June 2011

Accepted 4 October 2011

Published ahead of print 24 October 2011

Address correspondence to Walter Kolch, walter.kolch@ucd.ie.

\* Present address: Department of Pharmaceutical Chemistry and Chemical Biology, Aston University, Birmingham, United Kingdom.

Copyright © 2012, American Society for Microbiology. All Rights Reserved.

doi:10.1128/MCB.05770-11

## MATERIALS AND METHODS

**Materials.** Doxycycline, monoclonal mouse anti-VSV-G antibody, and anti-VSV-G agarose beads were from Sigma-Aldrich (Gillingham, United Kingdom), EGF was from Promega (Southampton, United Kingdom). Lipofectamine 2000 transfection reagent was from Invitrogen (Paisley, United Kingdom). Protease inhibitor cocktail tablets were from Roche Diagnostics (West Sussex, United Kingdom). Polyclonal goat eIF3a antibody, polyclonal rabbit EGFR antibody, monoclonal mouse SOS1 antibody, polyclonal rabbit c-Fos antibody, and monoclonal mouse  $\beta$ -actin antibody were from Santa Cruz (Heidelberg, Germany). Polyclonal rabbit SHC antibody and monoclonal mouse Ras antibody were from Upstate (Watford, United Kingdom). Monoclonal mouse Raf-1 antibody and monoclonal mouse Grb2 antibody were from BD (Oxford, United Kingdom). Monoclonal rabbit  $\beta$ -arrestin2 antibody, monoclonal mouse B-Raf antibody, polyclonal rabbit eIF3a antibody, polyclonal rabbit MEK1/2 antibody, monoclonal rabbit p44/42 mitogen-activated protein kinase (MAPK; ERK1/2) and polyclonal rabbit phospho-p44/42 MAPK (phospho-ERK1/2) antibodies were from Cell Signaling Technology (Hitchin, Hertfordshire, United Kingdom). Polyclonal rabbit anti-VSV-G antibody was generated in-house. pcDNA3-VSV- $\beta$ -arrestin2 and pcDNA3-Flag- $\beta$ -arrestin2 plasmids were constructed as described previously (44). The pc-DNA 5-HA-eIF3a expression vector was a gift from John W. B. Hershey (University of California).

**Cells.** HEK293 cells and derivatives, NIH 3T3 fibroblasts, and mouse embryonic fibroblasts (MEFs) derived from wild-type and  $\beta$ -arrestin-1/2 double knockout mice were maintained in Dulbecco modified Eagle medium (DMEM) supplemented with 0.292 g of L-glutamine/liter and 10% (vol/vol) fetal bovine serum (FBS). PC12 cells were maintained in DMEM plus 10% horse serum and 5% FBS.

**Generation of stable Flp-In T-REx HEK293 cells inducibly expressing VSV- $\beta$ -arrestin2.** VSV- $\beta$ -arrestin2 was generated by PCR and inserted into the KpnI-ApaI sites of pcDNA5/FRT/TO. The primers were CGAT GGT ACC GCC ACC ATG TAC ACC GAT ATA GAG ATG AAC CGC CTT GGA AAG GGG GAG AAA CCC GGG ACC AGG GT (forward with VSV-G sequence and KpnI site, underlined) and TGAT GGG CCC TCA ACA GAA CTG GTC ATA GTC CTC GT (reverse with ApaI site, underlined). To generate stable Flp-In T-REx HEK293 cells inducibly expressing VSV- $\beta$ -arrestin2, cells were transfected with a mixture containing VSV- $\beta$ -arrestin2 cDNA in pcDNA5/FRT/TO vector and the pOG44 vector (1:9) using Lipofectamine 2000 transfection reagent from Invitrogen, according to the manufacturer's instructions. Resistant clones were selected by replacing zeocin with 200  $\mu$ g of hygromycin B/ml, and the expression of VSV- $\beta$ -arrestin2 was examined by Western blotting with anti-VSV antibody. Clones were pooled to avoid clonal variation and maintained in DMEM without sodium pyruvate, 4,500 mg of glucose/liter, and L-glutamine supplemented with 10% (vol/vol) FBS, 1% antibiotic mixture, 100  $\mu$ g of zeocin/ml, and 10  $\mu$ g of blasticidin/ml. To induce the expression of VSV- $\beta$ -arrestin2, cells were treated with 1  $\mu$ g of doxycycline/ml for 24 h.

**Identification of  $\beta$ -arrestin2 binding proteins by mass spectrometry.** VSV- $\beta$ -arrestin2 was induced by 1  $\mu$ g of doxycycline/ml in Flp-in T-REx HEK293 cells. At 24 h after induction cells were harvested and resuspended in immunoprecipitation buffer (150 mM NaCl, 0.01 mM NaPO<sub>4</sub>, 2 mM EDTA, 0.5% Triton X-100, and 5% glycerol plus protease inhibitor cocktail tablets). Noninduced Flp-In T-REx 293 cells were used as negative control. The cell pellets were lysed and centrifuged for 15 min at 20,000  $\times$  g at 4°C, and the supernatant was transferred to fresh a tube with protein G/A-beads (Sigma) to preclear the samples. After 1 h at 4°C, the samples were recentrifuged at 20,000  $\times$  g for 1 min. Equal amounts of protein were incubated with anti-VSV-G agarose beads (Sigma) at 4°C for 2 h on a rotating wheel. Samples were subsequently washed four times with immunoprecipitation buffer. Proteins were eluted from beads by using 0.2 mg of VSV peptide (Sigma)/ml three times in immunoprecipitation buffer. The combined eluates were precipitated with 30% trichloroacetic acid at 4°C overnight. Precipitates were washed three times with

acetone and air dried. The precipitates were then resuspended in 6 M urea plus 0.1% N-octyl glucoside, diluted with 10 volumes of 25 mM ammonium bicarbonate, and digested with 20  $\mu$ g of sequencing-grade trypsin (Promega)/ml in 25 mM ammonium bicarbonate with 10 mM dithiothreitol overnight. The digestion was stopped by adding formic acid to 1%. Tryptic peptides were separated by a two-dimensional liquid chromatography (LC) system using stepwise elution from a cation exchange column and sequential fractionation of eluates on a Pepmap C<sub>18</sub> reversed-phase column (LC Packings, Bath, United Kingdom) by a 5 to 85% (vol/vol) acetonitrile gradient (in 0.5% [vol/vol] formic acid) run over 45 min. The flow rate was maintained at 0.2  $\mu$ l/min. The fractions were analyzed by online electrospray ionization mass spectrometry (MS) on a Q-STAR Pulsar-i MS/MS system. MS analysis was performed using a 3-s survey scan, followed by up to four MS/MS analyses of the most abundant peptides (3 s per peak) in information-dependent acquisition mode, choosing 2+ to 4+ ions above threshold of 30 counts, with dynamic exclusion for 180 s. The data generated from the Q-STAR Pulsar-i hybrid were analyzed by using Applied Biosystems Analyst QS (v1.1) software and the automated Matrix Science Mascot Daemon server (v2.1.06). Protein identifications were assigned using the Mascot search engine. In all cases, variable methionine oxidation was allowed in searches. An MS tolerance of 1.2 Da for MS and 0.4 Da for MS/MS analysis was used. The MS plus MS/MS data were searched against the NCBI nr public database. A match was considered significant if the MOWSE score was equal to or greater than 75. The proteins identified in both noninduced and induced samples were considered as no specific binding.

**siRNA-mediated gene silencing.** The small interfering RNA (siRNA) sequences targeting human eIF3a (Ambion) were as follows: CGAACCA AUUAUGUUGAAA-dTdT (sense) and UUUCAACAUAUUGGUUC G-dTdT (antisense). siRNAs against rat and mouse eIF3a were obtained from Ambion (AM16204) and Santa Cruz (sc-40551), respectively. The siRNA sequences targeting human  $\beta$ -arrestin2 were as follows: a mixture of AAGUCUCUGUGAGACAGUA-dTdT (sense), UACUGUCACAG AGACUU-dTdT (antisense), CGAACCAAGAUGACCAGGUA-dTdT (sense), and UACCUUGUCAUCUUGUUCG-dAdG (antisense). The Silencer control siRNA1 from Ambion was used as a negative control. siRNAs were transfected using Lipofectamine 2000 reagent according to the supplier's protocol.

**Coimmunoprecipitation studies.** Cells were harvested in coimmunoprecipitation buffer (150 mM NaCl, 0.01 mM NaPO<sub>4</sub>, 2 mM EDTA, 1 mM N-ethylmaleimide, 0.5% Triton X-100, and 5% glycerol plus protease inhibitor cocktail tablets) and processed as described above. Instead of elution with VSV, peptide samples were resolved by SDS-PAGE and subsequently immunoblotted to detect proteins of interest.

**BrdU incorporation.** Cells seeded on poly-lysine-coated coverslips were transfected with human eIF3a siRNA or control siRNA. At 24 h after transfection, the cells were serum starved for 48 h and stimulated with 20 ng of EGF/ml plus 20  $\mu$ M bromodeoxyuridine (BrdU) for another 6 h. The cells were then washed with phosphate-buffered saline (PBS) and fixed (90% ethanol, 5% acetic acid, 5% H<sub>2</sub>O) for 20 min. DNA was denatured with 2 M HCl at 37°C for 20 min and neutralized in 0.1 M Na<sub>2</sub>B<sub>4</sub>O<sub>7</sub> (pH 8.5) for 2 min. After three washes with PBS, the cells were blocked and permeabilized in 3% nonfat dry milk plus 0.15% Triton X-100 for 30 min and incubated with 1:500-diluted mouse anti-BrdU antibody (Sigma) in blocking buffer for 1 h. After another three PBS washes, the cells were incubated with 1:500 anti-mouse antibody-Alexa Fluor 594 (Molecular Probes) plus 10  $\mu$ g of Hoechst stain/ml for 1 h and subsequently washed with PBS for three times. Coverslips were mounted with Immu-Mount medium (Thermo). Images were collected with an epifluorescence microscope, and BrdU incorporation was quantified. BrdU-positive nuclei per total number of nuclei were counted from at least nine random microscope fields in each experiment. The statistical data came from three independent experiments.

**Focus formation assay.** NIH 3T3 cells were cultured in DMEM supplemented with 10% fetal calf serum. They were transfected with Lipo-

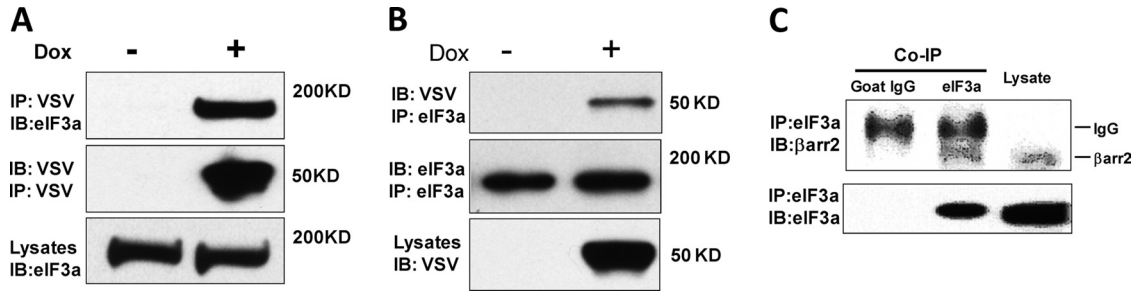


**FIG 1** Identification of eIF3a as a  $\beta$ -arrestin2 binding protein. (A) Expression of VSV-tagged  $\beta$ -arrestin2 in Flp-In T-Rex VSV- $\beta$ -arrestin2 cells was induced by 1  $\mu$ g of doxycycline/ml for 24 h. VSV- $\beta$ -arrestin2 was immunoprecipitated with mouse anti-VSV-G antibody covalently bound to agarose beads (Sigma) and blotted for associated eIF3a and immunoprecipitated VSV- $\beta$ -arrestin2 as indicated. (B) Aliquots of the lysates were immunoprecipitated with a goat anti-eIF3a antibody and blotted for associated VSV- $\beta$ -arrestin2 and immunoprecipitated eIF3a. Cell lysates (1,250  $\mu$ g) were used for immunoprecipitation, and 20  $\mu$ g of lysate per lane was loaded for Western blotting. (C) Endogenous eIF3a was immunoprecipitated from HEK293 cells with a goat anti-eIF3a antibody and examined for associated  $\beta$ -arrestin2 by Western blotting. Goat IgG (Sigma) was used as control. "IgG" refers to the IgG heavy chain.

fectamine (Invitrogen) according to the manufacturer's instructions. After 10 to 15 days, the cells were fixed with 100% methanol and stained with Giemsa blue, and transformed foci were counted.

**PC12 cell differentiation.** PC12 cells were transfected with rat eIF3a siRNA (Ambion, catalog no. AM16204) using an Amaxa Cell Line Nucleofector Kit V according to the supplier's protocol. The Silencer control siRNA1 (Ambion) was used as a negative control. At 48 h after transfection, the cells were treated with 20 ng of EGF or 100 ng of nerve growth factor (NGF)/ml. After 24 h, the cells were harvested and analyzed by Western blotting for ERK activation and quantitative PCR to assess the expression of neuronal marker genes (SCG-10 and VGF). For this, total cellular RNA was isolated by RNeasy minikit (Qiagen). A 1- $\mu$ g portion of total RNA was reverse transcribed by using random primers using Superscript III reverse transcriptase (Invitrogen). Differentiation markers SCG-10 and VGF mRNA were amplified by real-time PCR using the following primers: rat SCG-10, GCAATGGCCTACAAGGAAA (sense) and TTTCTGCAGACGTTCAATG (antisense); rat VGF, TACTGTTGCAGGCACTGGAC (sense) and AACGTTTTCCGACATTCGAG (antisense); and rat GAPDH, ATGGGAAGCTGGTCATCAAC (sense) and GGATGCAGGGATGATGTTCT (antisense). PCR-amplified sequences were quantified by using an ABI Prism 7900HT sequence detection system (Applied Biosystems) with a SYBR green gene expression assay. Relative quantification was achieved using the  $\Delta\Delta C_T$  method, which relates to internal control of GAPDH.

Statistical analysis was performed using a Student *t* test.

**RESULTS**

**$\beta$ -Arrestin2 interacts with eIF3a.** We identified eIF3a as a  $\beta$ -arrestin2-associated protein in a proteomic screen, where we

used human Flp-In T-Rex HEK293 cells engineered to express a doxycycline-inducible VSV-tagged  $\beta$ -arrestin2 in order to identify binding partners of  $\beta$ -arrestin2. Immunoprecipitation of VSV- $\beta$ -arrestin2 coprecipitated eIF3a (Fig. 1A) and, *vice versa*, immunoprecipitation of eIF3a coprecipitated VSV- $\beta$ -arrestin2 (Fig. 1B). The coprecipitations were strictly dependent on the induction of VSV- $\beta$ -arrestin2 expression supporting the specificity of the interaction. We also could coimmunoprecipitate endogenous eIF3a and  $\beta$ -arrestin2 proteins (Fig. 1C).

**Knockdown of  $\beta$ -arrestin2 or eIF3a prolongs EGF-induced ERK activation.** We had previously reported that  $\beta$ -arrestin2 mutants that are impaired to dimerize also show a diminished ability to bind to ERK and mediate ERK activation (44). Therefore, we tested the effects of  $\beta$ -arrestin2 downregulation on ERK activation (Fig. 2). We stimulated HEK293 cells with EGF and monitored ERK activation by blotting with phospho-specific antibodies detecting the activating phosphorylation sites (Fig. 2A). The downregulation of  $\beta$ -arrestin2 expression slightly augmented and significantly extended ERK activation by EGF (Fig. 2B).

In order to assess whether eIF3a was involved in this effect, we downregulated eIF3a and examined ERK activation (Fig. 3A). Similar to  $\beta$ -arrestin2, eIF3a knockdown caused a slight increase in the peak of ERK activity and a significant extension of the duration of ERK activation (Fig. 3B). These results suggested that eIF3a may be involved in mediating the suppressive effects of  $\beta$ -arrestin2 on the EGF-stimulated ERK pathway. Since

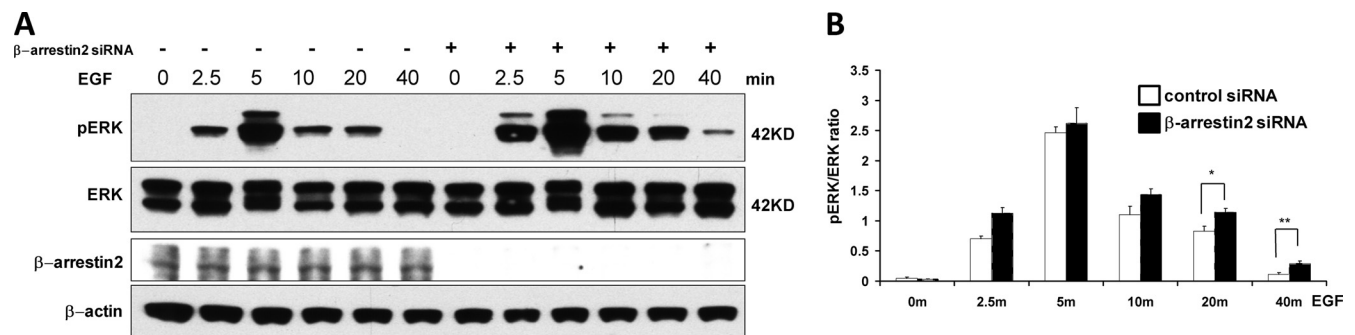


**FIG 2** Knockdown of  $\beta$ -arrestin2 causes sustained ERK activity in response to EGF. (A)  $\beta$ -Arrestin2 was knocked down in HEK293 cells with siRNA. The  $\beta$ -arrestin2 knockdown efficiency was monitored by Western blotting with  $\beta$ -actin as loading control. Cells were treated with EGF for the indicated time points, and ERK activation was examined by blotting with a phospho-specific antibody. (B) The ratio of phospho-ERK to total ERK (pERK/ERK) was quantified by densitometric evaluation of Western blots. The data represent the means  $\pm$  the standard errors of the mean (SEM) of six independent experiments. \*, *P* < 0.05; \*\*, *P* < 0.01.

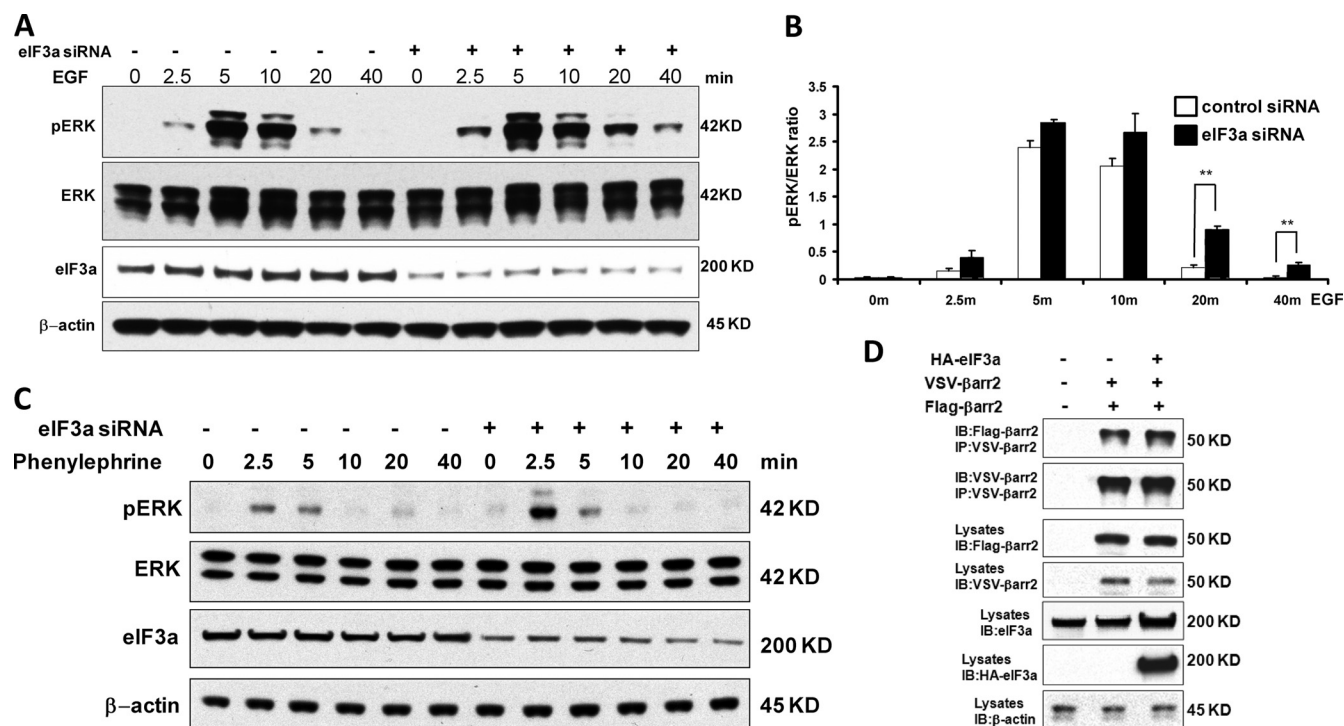


**FIG 3** Knockdown of eIF3a causes sustained ERK activity in response to EGF. (A) eIF3a was knocked down in HEK293 cells with siRNA, and knockdown efficiency was monitored by Western blotting with  $\beta$ -actin as a loading control. Cells were treated with EGF for the indicated time points, and ERK activation was examined by blotting with a phospho-specific antibody. (B) The ratio of phospho-ERK to total ERK (pERK/ERK) was quantified by densitometric evaluation of Western blots. The data represent the means  $\pm$  the SEM of six independent experiments. \*\*,  $P < 0.01$ . (C) eIF3a was knocked down in HEK293 cells with siRNA, and knockdown efficiency was monitored by Western blotting. Serum-starved cells were treated with the  $\alpha_{1B}$ -adrenergic receptor agonist phenylephrine ( $10^{-4}$  M) for the indicated time points, and phospho-ERK was detected by Western blotting. The same membrane was reprobed for total ERK and  $\beta$ -actin as loading controls. (D) Overexpression of eIF3a does not affect  $\beta$ -arrestin2 dimerization. HEK293 cells were cotransfected with VSV- $\beta$ -arrestin2, Flag- $\beta$ -arrestin2 and HA-eIF3a as indicated. The corresponding empty vectors were used as a control (in the lanes labeled “-”). At 24 h after transfection, VSV- $\beta$ -arrestin2 was immunoprecipitated and blotted with antibodies against the VSV and Flag tags. The expression of transfected proteins was monitored by blotting cell lysates.  $\beta$ -Actin was used as loading control.

$\beta$ -arrestin2 is usually associated with the regulation of G-protein-coupled receptor (GPCR) signaling (9, 35), we also tested whether ERK activation by phenylephrine, a ligand of the  $\alpha_{1B}$ -adrenergic receptor, was influenced by eIF3a. Downregulation of eIF3a by siRNA did not change the kinetics of ERK activation by phenylephrine but increased the peak amplitude (Fig. 3C). Thus, we set out to explore the mechanism of eIF3a-mediated ERK regulation. eIF3a did not affect the ability of  $\beta$ -arrestin2 to dimerize (Fig. 3D), which we previously reported to be important for the regulation of ERK signaling by  $\beta$ -arrestin2 (44). Therefore, we investigated other mechanisms by which eIF3a may regulate ERK activation.

**$\beta$ -Arrestin2 modulates binding of eIF3a to selected components of the ERK pathway.** Since eIF3a modulated the activation of ERK in response to EGF, we tested whether eIF3a could interact with components of the ERK pathway. For this purpose, we immunoprecipitated endogenous eIF3a and assessed the coprecipitation of the EGFR, SHC, Grb2, SOS, Ras, Raf-1, B-Raf, MEK, and ERK (Fig. 4A). An unrelated, species-matched antibody was used as a control. Specific interactions were observed between eIF3a and SHC and between eIF3a and Raf-1. Interestingly, B-Raf did not interact with eIF3a, suggesting that the interaction is Raf isoform specific. We then examined the influence of  $\beta$ -arrestin2 on the interaction of eIF3a with SHC and Raf-1 (Fig. 4B). Although the induction of  $\beta$ -arrestin2 expression had no influence on the

interaction between eIF3a and SHC, it enhanced the interaction between eIF3a and Raf-1 (Fig. 4B). The role of  $\beta$ -arrestin2 in promoting the interaction between eIF3a and Raf-1 was confirmed by using  $\beta$ -arrestin1/2 knockout cells. The association between Raf-1 and eIF3a was severely reduced in  $\beta$ -arrestin1/2 knockout cells (Fig. 4C). In summary, these data suggested that eIF3a may sequester Raf-1 from EGF activation. Therefore, we focused our further investigations on the interaction and functional relationship between eIF3a and Raf-1.

**eIF3a binding to Raf-1 is regulated by EGF.** The hypothesis that eIF3a may sequester Raf-1 from EGF-mediated activation predicted that EGF stimulation should diminish this interaction. This was indeed the case (Fig. 5A). Importantly, EGF caused an early dissociation of Raf-1 from eIF3a and a reassociation at later time points, which closely corresponded to the time course of ERK activation. In addition, the dissociation of Raf-1 from eIF3a was dependent on the EGF dose (Fig. 5B). Again, the progressive disruption of the eIF3a-Raf-1 complex with increasing EGF doses was mirrored by an increase in ERK activation (Fig. 5B). Interestingly, the fraction of Raf-1 that coimmunoprecipitated with eIF3a was phosphorylated on S259 and stayed phosphorylated on this site after EGF treatment (Fig. 5C). S259 phosphorylation is inhibitory for Raf-1 kinase activity and needs to be dephosphorylated for Raf-1 activation to take place (1, 2, 12, 24). The dephosphor-

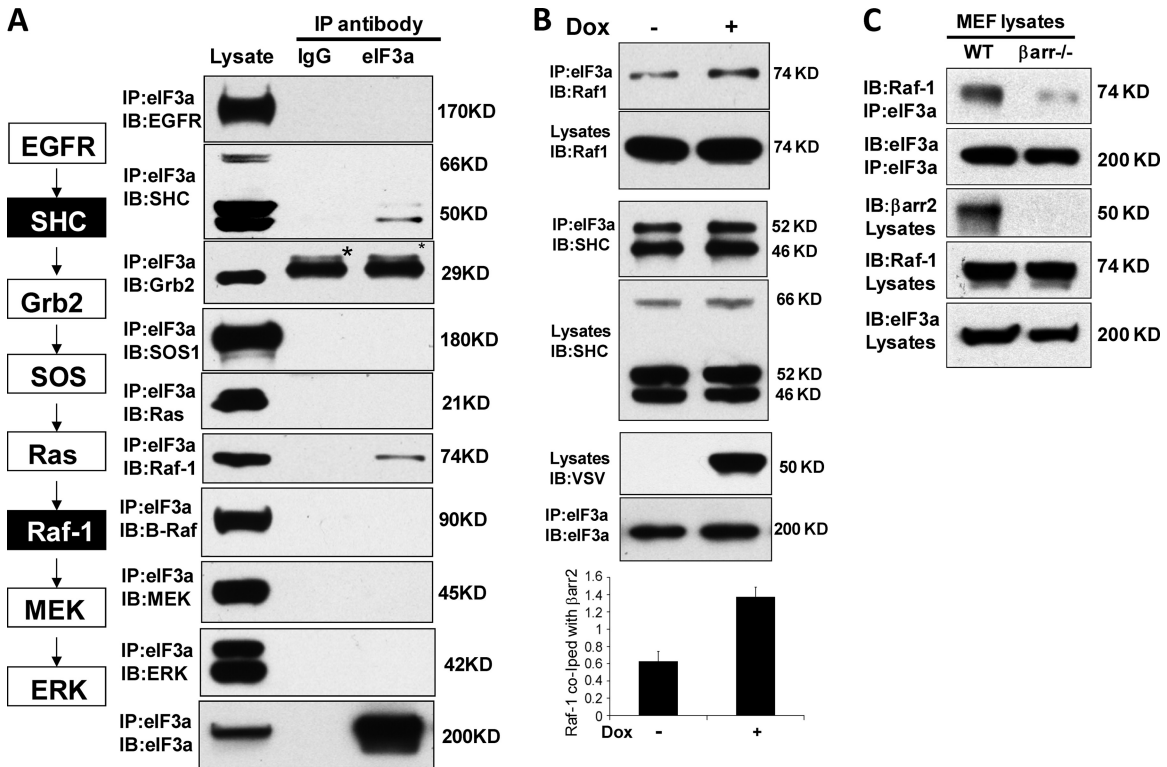


**FIG 4** Binding of eIF3a to protein components of the EGFR-ERK pathway. (A) Endogenous eIF3a was immunoprecipitated from HEK293 cells with a goat anti-eIF3 antibody and examined for associated proteins using the indicated antibodies. Goat IgG (Sigma) was used as control. The proteins examined and their positions in the pathway are schematically shown on the left with the proteins coprecipitating with eIF3a indicated in black boxes. The bands labeled with asterisks in the Grb2 blot are IgG light chains detected by the secondary antibody. (B)  $\beta$ -Arrestin2 increases eIF3a binding to Raf-1 but not to SHC. Flp-In T-REX VSV- $\beta$ -arrestin2 cells were induced with 1  $\mu$ g of doxycycline (Dox)/ml or vehicle control for 24 h. Induction of VSV- $\beta$ -arrestin2 was monitored by Western blotting with anti-VSV antibody. eIF3a immunoprecipitates were examined for coprecipitating SHC (left panel) and Raf-1 (right panel). A densitometric quantitation (arbitrary units) of Raf-1 binding to eIF3a is shown below, representing the means  $\pm$  the SEM from three independent experiments. \*,  $P < 0.05$ . (C) Endogenous eIF3a was immunoprecipitated from MEF wild-type cells or MEF  $\beta$ -arrestin1/2 knockout cells, and the associated Raf-1 was examined by Western blotting.

ylation of S259 is required for the subsequent phosphorylation of S338 (12, 13), which is essential for Raf-1 kinase activation (14). In response to EGF treatment Raf-1 associated with eIF3a did not become dephosphorylated on S259 and did not become phosphorylated on S338. In contrast, S259 dephosphorylation and S338 phosphorylation were observable in cell lysates (Fig. 5C). These data indicate that the binding of eIF3a to Raf-1 prevents the Raf-1 activation cycle and further corroborate the hypothesis that eIF3a binding impedes the activation of Raf-1 and the downstream ERK pathway.

**eIF3a regulates ERK signaling and its biological effects.** In response to stimulation of angiotensin II type 1a receptors  $\beta$ -arrestins have been shown to function as scaffolds that selectively promote the activation of the ERK pathway in the cytosol, but not in the nucleus (41). Therefore, we investigated whether eIF3a may have a similarly compartmentalized effect on ERK signaling. We first assayed the effect of eIF3a on the induction of c-Fos, an early gene that is a classic transcriptional target of ERK signaling (25). Downregulation of eIF3a increased the basal levels c-Fos protein and enhanced the induction of c-Fos protein expression by EGF (Fig. 6A), indicating that eIF3a downregulation also promotes ERK nuclear signaling.

In order to test whether the enhanced ERK signaling enabled by eIF3a downregulation also has biological effects, we examined

DNA synthesis. Although basal DNA synthesis was unchanged, eIF3a downregulation caused a small, but significant increase in EGF-stimulated DNA synthesis.

These data suggested that eIF3a modulates the biochemical activation of ERK, as well as its biological effects in HEK293 cells. In order to evaluate this hypothesis in other cell systems, we examined the effects of eIF3a on ERK activation and ERK-dependent phenotypic cellular outcomes, such as neuronal differentiation in PC12 cells and transformation in NIH 3T3 cells (Fig. 7). Sustained ERK signaling is essential for the differentiation of PC12 into neuronal cells (31, 42). In PC12 cells the downregulation of eIF3a in PC12 enhanced EGF- and NGF-induced ERK phosphorylation (Fig. 7A) and the induction of the neuronal differentiation markers SCG-10 and VGF (6, 28, 43) by NGF (Fig. 7B). Unfortunately, we could not reliably assess differences in neurite extension, presumably because of additional effects of the eIF3a knockdown on protein synthesis, which may interfere with neurite outgrowth. As a different biological system, we examined transformation as assayed by focus formation in the classic NIH 3T3 cell system (23). In NIH 3T3 cells we could overexpress and knockdown eIF3a. The knockdown of eIF3a enhanced ERK phosphorylation and focus formation, while its overexpression reduced RasV12 induced ERK phosphorylation and focus formation (Fig. 7C).

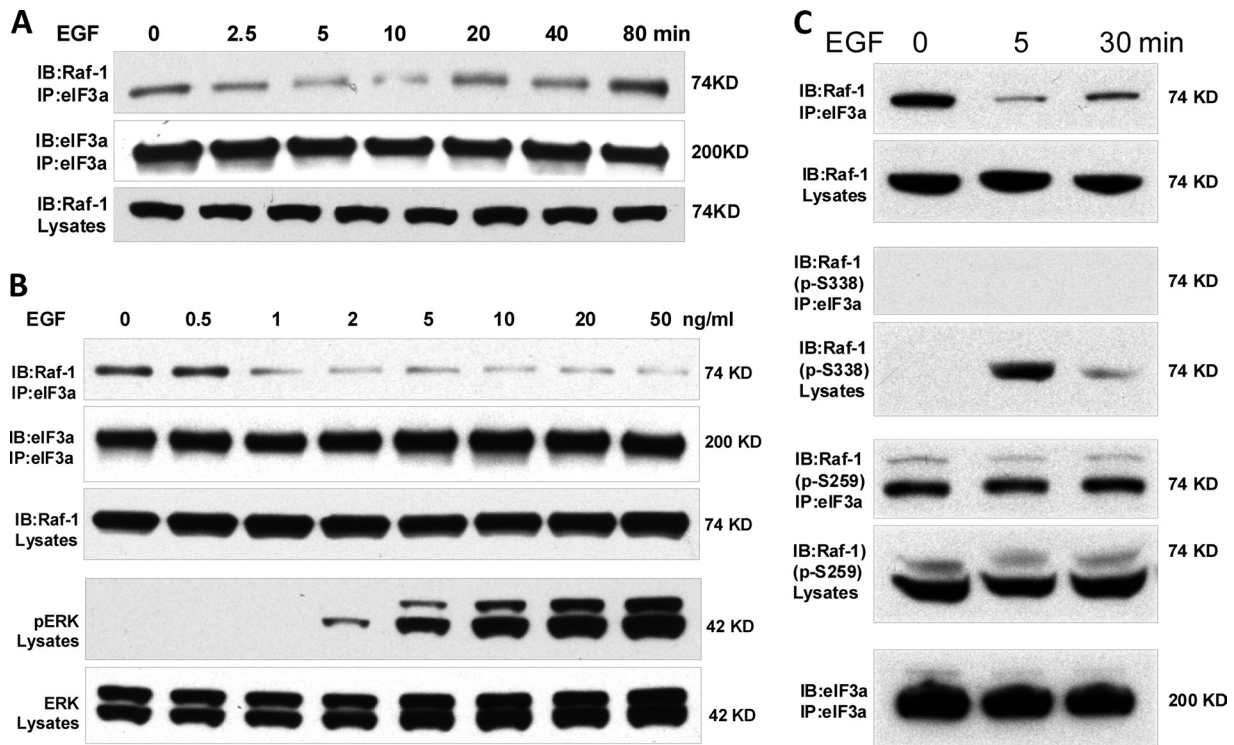


**FIG 5** EGF regulation of eIF3a–Raf-1 association correlates with ERK pathway activation. (A) HEK293 cells were serum starved overnight and treated with 20 ng of EGF/ml for the times indicated. Endogenous eIF3a was immunoprecipitated and examined for associated Raf-1 by Western blotting. The blots shown are representative of three independent experiments. (B) Serum-starved HEK293 cells were stimulated with increasing doses of EGF for 5 min. The eIF3a–Raf-1 association and ERK activation was assessed by Western blotting. The data are representative of three independent experiments. (C) eIF3a was immunoprecipitated from EGF stimulated HEK293 cells. Raf-1 bound to eIF3a was examined for phosphorylation of the inhibitory S259 and activating S338 sites.

In summary, these data confirm that eIF3a has a suppressive effect on signaling through the ERK pathway and the biological outcomes thereof.

**DISCUSSION**

Our results suggest that  $\beta$ -arrestin2 can functionally interfere with the activation of the ERK pathway by EGF through enhancing the binding of eIF3a to Raf-1. These data add two new aspects to the regulation of Raf and ERK signaling, namely, in revealing novel regulatory roles for  $\beta$ -arrestin2 and eIF3a.

$\beta$ -Arrestin1 and  $\beta$ -arrestin2 were originally discovered as pro-

teins that terminate GPCR signaling but have turned out to be multifunctional proteins that play critical roles in coordinating GPCR- and EGFR-dependent signaling pathways (4, 8, 10, 35). The relationship mainly has been explored from the role  $\beta$ -arrestins play in cross-regulating EGFR signaling after stimulation of a GPCR. The results suggest a complicated interplay, where  $\beta$ -arrestin1 and  $\beta$ -arrestin2 can have different and antagonistic roles in the regulation of the ERK pathway (3, 18, 19). Our results suggest that  $\beta$ -arrestin2 can impede ERK pathway activation by EGF, while downregulation of  $\beta$ -arrestin2 enhances ERK activation. This regulation pertains to the duration of ERK signaling

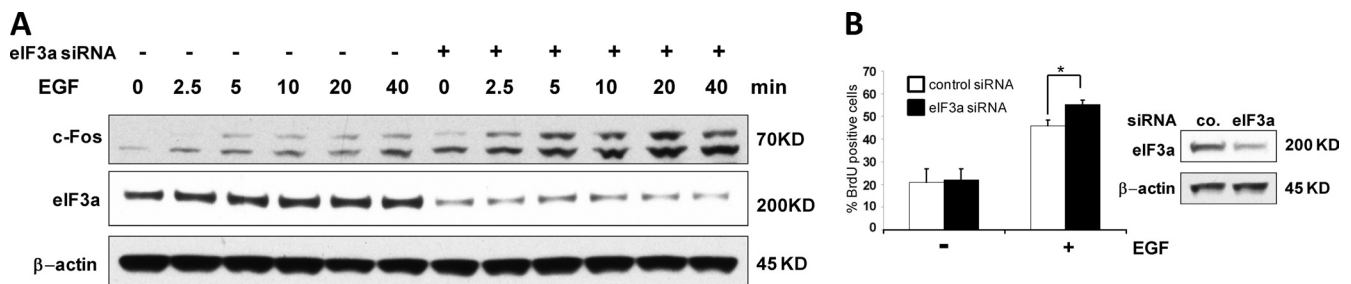


**FIG 6** Knockdown of eIF3a enhances EGF induced c-Fos expression and DNA synthesis. (A) HEK293 cells were transfected with siRNA against eIF3a, serum starved, and treated with 20 ng of EGF/ml for the indicated time points. Induction of c-Fos protein and levels of eIF3a were assessed by Western blotting.  $\beta$ -Actin served as a loading control. The data are representative of three independent experiments. (B) The effects of eIF3a knockdown on DNA synthesis in serum-starved and EGF-treated HEK293 cells was measured by BrdU incorporation. The experiment was performed three times, and >400 cells were counted in each case. The data are means  $\pm$  the SEM. \*,  $P < 0.05$ . The eIF3a knockdown efficiency was monitored by Western blotting.

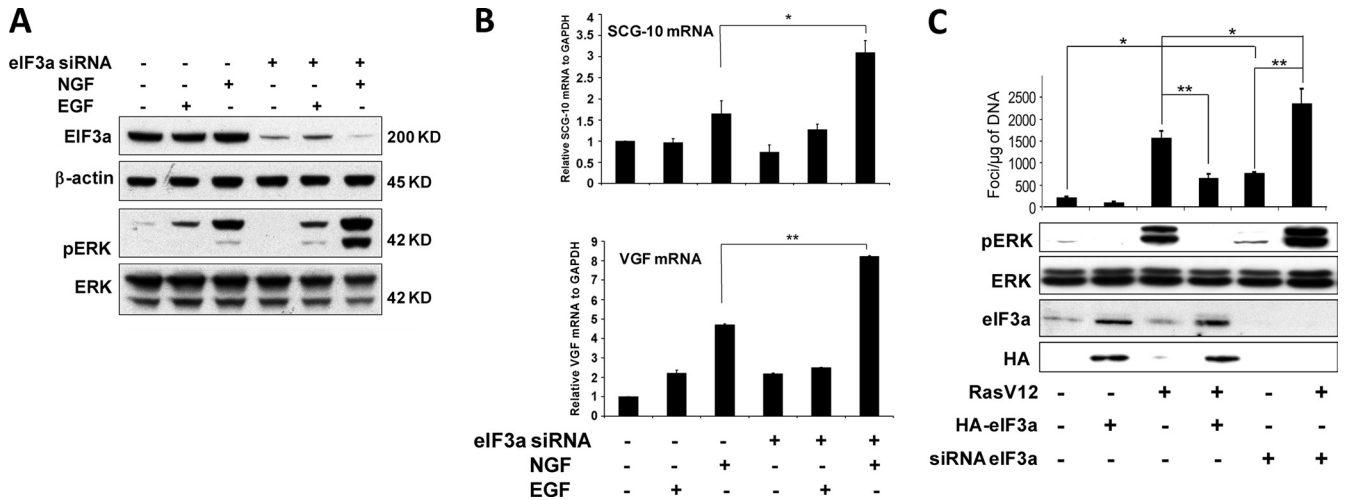


**FIG 7** Knockdown of eIF3a enhances the expression of differentiation markers in PC12 cell and focus formation in NIH 3T3 cells. (A) PC12 cells were transfected with siRNA against rat eIF3a. At 48 h later cells were treated with EGF (20 ng/ml) or NGF (100 ng/ml) for 24 h. ERK phosphorylation was monitored by Western blotting. Knockdown efficiency was monitored by Western blotting with  $\beta$ -actin as loading control. (B) In parallel, the mRNA levels of the neuronal differentiation markers SCG-10 and VGF were monitored by real-time PCR using GAPDH as an internal control. The data represent the means  $\pm$  the SEM of three independent experiments. \*,  $P < 0.05$ ; \*\*,  $P < 0.01$ . (C) NIH 3T3 were cotransfected with either empty vector, HA-tagged eIF3a, scrambled (–) or eIF3a siRNA, and RasV12 as indicated. Cells were grown for 2 weeks and examined for the formation of transformed foci. Indicated values represent number of foci/ $\mu$ g of DNA  $\pm$  the SEM ( $n = 6$ ). \*,  $P < 0.05$ ; \*\*,  $P < 0.01$ . In parallel, 10  $\mu$ g of cellular extracts was analyzed 1 week after transfection by Western blotting with antibodies against the indicated proteins.

rather than to peak activation, and while statistically significant it is quite subtle. These properties may explain why it has not been observed in previous studies.

Differences in spatial and temporal components of ERK activation can lead to profoundly distinct functional effects (26, 33, 38). Our results also suggest that eIF3a can exert specific regulatory effects on the kinetics of ERK activation through its interaction with  $\beta$ -arrestin2. Specifically, this is mediated by  $\beta$ -arrestin2 binding to eIF3a, which serves to enhance the binding of eIF3a to Raf-1. Since  $\beta$ -arrestin2 can act as a scaffold that facilitates the assembly of the Raf-1/MEK/ERK kinase signaling cascade (29), and eIF3a also can bind Raf-1, then the enhancing effects of  $\beta$ -arrestin2 on the eIF3a–Raf-1 interaction may simply be due to the formation of a higher-order complex where binding affinities are cooperatively stabilized. However, while  $\beta$ -arrestin2 promotes ERK activation (29), eIF3a interferes with it. Thus, the interactions between Raf-1,  $\beta$ -arrestin2, and eIF3a may occur in different protein complexes, different subcellular compartments or on different time frames. Distinguishing between these possibilities is technically extremely challenging and will require future evaluation as and when technologies develop to map ternary protein complexes with high spatial resolution. Nevertheless, our data provide mechanistic insights showing that the mechanism of ERK pathway inhibition by eIF3a is the interference with Raf-1 activation, as reflected by a lack of dephosphorylation of the inhibitory residue S259 and failure to phosphorylate S338 in Raf-1. These changes in phosphorylation are Ras dependent and take place at the membrane (12–14), suggesting that eIF3a interference operates at the membrane and not at the endosome level, where  $\beta$ -arrestin2 is thought to scaffold the Raf-1/MEK/ERK pathway (29). Interestingly, eIF3a localization has been described to include the plasma membrane (34), which is clearly compatible with a mechanism of interference with Raf-1 activation at the plasma membrane.

In addition to its role in protein translation, eIF3a has been suggested to have other functions, especially in cancer, although the findings are contradictory as to whether eIF3a promotes or counteracts cellular transformation (36). In cell culture systems, the overexpression of different eIF3a subunits, including eIF3a, was described to transform cells (46). This finding is in contrast to our results, which suggest that eIF3a downregulation promotes and eIF3a overexpression counteracts Ras mediated transformation of NIH 3T3 cells. The reasons for these discrepant observations may be intricate and multifactorial, but a plausible explanation is offered by our results that the binding of eIF3a to Raf-1 is highly dependent on scaffolding by  $\beta$ -arrestin2. Thus, as with any scaffolded process, the result will depend on the expression stoichiometry of the scaffold and its binding partners. eIF3a was found overexpressed in cancers of breast, lung, cervix, esophagus, stomach, and colon (21, 36, 40). In keeping with a cancer-promoting role, the overexpression of several eIF3 subunits, including eIF3a, was shown to transform NIH 3T3 fibroblasts (46). However, further studies in cervical, esophageal, and gastric cancer demonstrated that eIF3a overexpression was associated with a better prognosis (36). These findings correlate with our results suggesting that the role of eIF3a in malignancy is more differentiated and require further, highly quantitative studies. In a more global context, these observations give rise to the intriguing hypothesis that mitogenic signaling and the protein translation machinery may be connected by a regulatory circuit whereby free subunits of translation factors suppress mitogenic signaling pathways in order to ensure that the cellular response to mitogens remains coupled with the cellular capacity of protein production.

**ACKNOWLEDGMENTS**

This study was supported by Medical Research Council grant G0400053/69186 and by Science Foundation Ireland under grant 06/CE/B1129.

## REFERENCES

- Abraham D, et al. 2000. Raf-1-associated protein phosphatase 2A as a positive regulator of kinase activation. *J. Biol. Chem.* 275:22300–22304.
- Adams DG, et al. 2005. Positive regulation of Raf1-MEK1/2-ERK1/2 signaling by protein serine/threonine phosphatase 2A holoenzymes. *J. Biol. Chem.* 280:42644–42654.
- Ahn S, Wei H, Garrison TR, Lefkowitz RJ. 2004. Reciprocal regulation of angiotensin receptor-activated extracellular signal-regulated kinases by beta-arrestins 1 and 2. *J. Biol. Chem.* 279:7807–7811.
- Baillie GS, Houslay MD. 2005. Arrestin times for compartmentalized cAMP signaling and phosphodiesterase-4 enzymes. *Curr. Opin. Cell Biol.* 17:129–134.
- Calvo F, Agudo-Ibanez L, Crespo P. 2010. The Ras-ERK pathway: understanding site-specific signaling provides hope of new anti-tumor therapies. *Bioessays* 32:412–421.
- D'Arcangelo G, Halegoua S. 1993. A branched signaling pathway for nerve growth factor is revealed by Src-, Ras-, and Raf-mediated gene inductions. *Mol. Cell. Biol.* 13:3146–3155.
- Damoc E, et al. 2007. Structural characterization of the human eukaryotic initiation factor 3 protein complex by mass spectrometry. *Mol. Cell Proteomics* 6:1135–1146.
- Defea K. 2008. Beta-arrestins and heterotrimeric G-proteins: collaborators and competitors in signal transduction. *Br. J. Pharmacol.* 153(Suppl. 1):S298–S309.
- DeFea KA. 2011. Beta-arrestins as regulators of signal termination and transduction: how do they determine what to scaffold? *Cell Signal.* 23:621–629.
- DeWire SM, Ahn S, Lefkowitz RJ, Shenoy SK. 2007. Beta-arrestins and cell signaling. *Annu. Rev. Physiol.* 69:483–510.
- Dhillon AS, Hagan S, Rath O, Kolch W. 2007. MAP kinase signalling pathways in cancer. *Oncogene* 26:3279–3290.
- Dhillon AS, Meikle S, Yazici Z, Eulitz M, Kolch W. 2002. Regulation of Raf-1 activation and signalling by dephosphorylation. *EMBO J.* 21:64–71.
- Dhillon AS, von Kriegsheim A, Grindlay J, Kolch W. 2007. Phosphatase and feedback regulation of Raf-1 signaling. *Cell Cycle* 6:3–7.
- Diaz B, et al. 1997. Phosphorylation of Raf-1 serine 338-serine 339 is an essential regulatory event for Ras-dependent activation and biological signaling. *Mol. Cell. Biol.* 17:4509–4516.
- Dong Z, Liu LH, Han B, Pincheira R, Zhang JT. 2004. Role of eIF3 p170 in controlling synthesis of ribonucleotide reductase M2 and cell growth. *Oncogene* 23:3790–3801.
- Dong Z, Zhang JT. 2003. EIF3 p170, a mediator of mimosine effect on protein synthesis and cell cycle progression. *Mol. Biol. Cell* 14:3942–3951.
- Dong Z, Zhang JT. 2006. Initiation factor eIF3 and regulation of mRNA translation, cell growth, and cancer. *Crit. Rev. Oncol. Hematol.* 59:169–180.
- Gesty-Palmer D, et al. 2006. Distinct beta-arrestin- and G protein-dependent pathways for parathyroid hormone receptor-stimulated ERK1/2 activation. *J. Biol. Chem.* 281:10856–10864.
- Gesty-Palmer D, El Shewy H, Kohout TA, Luttrell LM. 2005.  $\beta$ -Arrestin 2 expression determines the transcriptional response to lysophosphatidic acid stimulation in murine embryo fibroblasts. *J. Biol. Chem.* 280:32157–32167.
- Hasek J, et al. 2000. Rpg1p, the subunit of the *Saccharomyces cerevisiae* eIF3 core complex, is a microtubule-interacting protein. *Cell Motil. Cytoskeleton* 45:235–246.
- Haybaeck J, et al. 2010. Overexpression of p150, a part of the large subunit of the eukaryotic translation initiation factor 3, in colon cancer. *Anticancer Res.* 30:1047–1055.
- Hinnebusch AG. 2006. eIF3: a versatile scaffold for translation initiation complexes. *Trends Biochem. Sci.* 31:553–562.
- Jainchill JL, Aaronson SA, Todaro GJ. 1969. Murine sarcoma and leukemia viruses: assay using clonal lines of contact-inhibited mouse cells. *J. Virol.* 4:549–553.
- Jaumot M, Hancock JF. 2001. Protein phosphatases 1 and 2A promote Raf-1 activation by regulating 14-3-3 interactions. *Oncogene* 20:3949–3958.
- Karin M. 1996. The regulation of AP-1 activity by mitogen-activated protein kinases. *Philos Trans. R. Soc. Lond. B Biol. Sci.* 351:127–134.
- Kholodenko BN, Hancock JF, Kolch W. 2010. Signalling ballet in space and time. *Nat. Rev. Mol. Cell. Biol.* 11:414–426.
- Lin L, Holbro T, Alonso G, Gerosa D, Burger MM. 2001. Molecular interaction between human tumor marker protein p150, the largest subunit of eIF3, and intermediate filament protein K7. *J. Cell Biochem.* 80:483–490.
- Luc PV, Wagner JA. 1997. Regulation of the neural-specific gene VGF in PC12 cells: identification of transcription factors interacting with NGF-responsive elements. *J. Mol. Neurosci.* 8:223–241.
- Luttrell LM, et al. 2001. Activation and targeting of extracellular signal-regulated kinases by beta-arrestin scaffolds. *Proc. Natl. Acad. Sci. U. S. A.* 98:2449–2454.
- MacDonald JJ, Verdi JM, Meakin SO. 1999. Activity-dependent interaction of the intracellular domain of rat trkA with intermediate filament proteins, the beta-6 proteasomal subunit, Ras-GRF1, and the p162 subunit of eIF3. *J. Mol. Neurosci.* 13:141–158.
- Marshall CJ. 1995. Specificity of receptor tyrosine kinase signaling: transient versus sustained extracellular signal-regulated kinase activation. *Cell* 80:179–185.
- McKay MM, Morrison DK. 2007. Integrating signals from RTKs to ERK/MAPK. *Oncogene* 26:3113–3121.
- Murphy LO, Blenis J. 2006. MAPK signal specificity: the right place at the right time. *Trends Biochem. Sci.* 31:268–275.
- Pincheira R, Chen Q, Huang Z, Zhang JT. 2001. Two subcellular localizations of eIF3 p170 and its interaction with membrane-bound microfilaments: implications for alternative functions of p170. *Eur. J. Cell Biol.* 80:410–418.
- Rajagopal S, Rajagopal K, Lefkowitz RJ. 2010. Teaching old receptors new tricks: biasing seven-transmembrane receptors. *Nat. Rev. Drug Discov.* 9:373–386.
- Saletta F, Rahmanto YS, Richardson DR. 2010. The translational regulator eIF3a: the tricky eIF3 subunit! *Biochim. Biophys. Acta* 1806:275–286.
- Severin FF, et al. 1997. A major 170-kDa protein associated with bovine adrenal medulla microtubules: a member of the centrosomin family? *FEBS Lett.* 420:125–128.
- Shankaran H, Wiley HS. 2010. Oscillatory dynamics of the extracellular signal-regulated kinase pathway. *Curr. Opin. Genet. Dev.* 20:650–655.
- Shaul YD, Seger R. 2007. The MEK/ERK cascade: from signaling specificity to diverse functions. *Biochim. Biophys. Acta* 1773:1213–1226.
- Silvera D, Formenti SC, Schneider RJ. 2010. Translational control in cancer. *Nat. Rev. Cancer* 10:254–266.
- Tohgo A, Pierce KL, Choy EW, Lefkowitz RJ, Luttrell LM. 2002.  $\beta$ -Arrestin scaffolding of the ERK cascade enhances cytosolic ERK activity but inhibits ERK-mediated transcription following angiotensin AT1a receptor stimulation. *J. Biol. Chem.* 277:9429–9436.
- von Kriegsheim A, et al. 2009. Cell fate decisions are specified by the dynamic ERK interactome. *Nat. Cell Biol.* 11:1458–1464.
- Wu YY, Bradshaw RA. 1996. Synergistic induction of neurite outgrowth by nerve growth factor or epidermal growth factor and interleukin-6 in PC12 cells. *J. Biol. Chem.* 271:13033–13039.
- Xu TR, et al. 2008. Mutations of beta-arrestin 2 that limit self-association also interfere with interactions with the beta2-adrenoceptor and the ERK1/2 MAPKs: implications for  $\beta$ 2-adrenoceptor signaling via the ERK1/2 MAPKs. *Biochem. J.* 413:51–60.
- Yoon S, Seger R. 2006. The extracellular signal-regulated kinase: multiple substrates regulate diverse cellular functions. *Growth Factors* 24:21–44.
- Zhang L, Pan X, Hershey JW. 2007. Individual overexpression of five subunits of human translation initiation factor eIF3 promotes malignant transformation of immortal fibroblast cells. *J. Biol. Chem.* 282:5790–5800.